DOI: https://doi.org/10.68732/607efe1746653317

ISBN: 978-9989-2053-6-1

Integrated Petrographic and Sorption Analysis of Pore Morphology in Sub-bituminous Coals

A. Tripathy
Indian Institute of Technology (ISM) Dhanbad, Dhanbad, Jharkhand, 826004, India
ashutosh@iitism.ac.in
0000-0001-7253-2960

M. Mazumder
Indian Institute of Technology (ISM) Dhanbad, Dhanbad, Jharkhand, 826004, India
0009-0005-6020-3656

T.N. Singh
Indian Institute of Technology, Patna, Bihta, Dayalpur, Bihar, 801106, India
0009-0005-7159-631X

Abstract

The generation and migration of CBM occur in the nanoscale pore found in coals. Nonetheless, the extreme compactness and multifaceted characteristics of nanopores remain poorly understood in terms of their morphology. In this study, coal samples were collected from Jharia coalfield, India. 2D image analysis, geochemical analysis, and low-pressure N_2 adsorption (LPNA) studies were used to examine the morphological parameters of the pore that influence it. According to the petrographic analysis, vitrinite is the dominant group among all macerals in samples (mean 62%), with a notable proportion of liptinite (24%) maceral group, whereas the concentration of inertinite group is the lowest (12.5%). Values of Vitrinite reflectance range from 0.54% to 0.61%, whereas ash content varies between 45.9 and 55.1%, volatile matter ranges from 31.1 to 37.1%, and moisture content varies from 7.1 to 9.2%, indicating that Jharia coal is of sub- bituminous 'B' rank. The primary pore types identified by the microphotographic image observation are the interparticle pores, the intraparticle pores, and the microcracks. Volume of pore ranges from 0.000277 to 0.029754 cm^3 /g, whereas values of SSA range between and m^2/g. From rock-eval pyrolysis result, value of the HI ranges from 201 to 209 mg HC/g TOC, whereas the T_{max} ranges from 423 to 429. HI vs. T_{max} data indicates that samples are thermally mature and type II kerogen in nature. TOC varies from 63.59% to 66.8% wt%. From a rock mechanical standpoint, the heterogeneity in pore morphology and maceral composition indicates variable stress sensitivity and deformation behavior under in-situ conditions. From the above results, it can be shown that total organic carbon is positively and negatively related with pore parameters, indicating that TOC has the greatest influence on pore characteristics and suggesting a significant hydrocarbon potential. Our results strengthen the experimental basis for understanding coal nanopore structure.

Keywords

Coal, Maturity, Coal Bed Methane, Maceral, Organic matter.

1 Introduction

CBM (Coal Bed Methane)gas produced by thermogenic and/or biogenic processes is mostly stored in situ as free gas (found in pores, cracks and fractures) and adsorbed gas (found on organic matter) (Curtis, 2002; Jarvie et al., 2007). Due to the presence of a wide variety of pore sizes with different shapes, types and origins, pore system is usually complex and heterogeneous in coal (Loucks et al., 2009, 2012; Clarkson et al., 2013). On the basis of relationship between pore and mineral particles, coal matrix-related pores can be categorized as interparticle pores between mineral grains and crystals, intraparticle pores within mineral particles, and organic matter pores (Loucks et al., 2012). As it may have negative impact on the CBM exploration in reservoir, it is imperative to precisely characterise the pore development characteristics in various organic materials.

The properties and controlling parameters of pore morphology in reservoir rocks have been determined by several researchers in recent years. For example, Loucks et al. (2009, 2012) noted that thermal maturity primarily regulates the development of organic matter (OM) pores. According to Milliken et al. (2013) and Jarvie et al. (2007), Type I and type II kerogen have a greater capacity to produce hydrocarbons than type III kerogen, which may make them more susceptible to pore generation. According to Yang et al. (2014), Total organic carbon (TOC) regulates specific surface area and methane adsorption ability of coal and coal measure rocks. Recent studies have stated that maceral composition may have an impact on the heterogeneous development of OM pores (Tripathy et al., 2026; Cao et al., 2018; Liu et al., 2017; Ardakani et al., 2018; Wood et al., 2018). The Permian coal reservoir, containing Barakar formation and Raniganj formation in Damodar valley is regarded as a desirable target for CBM exploration (Du et al., 2015; Pan et al., 2015, Mazumder et al., 2024b, 2024c,2026), because of its wide regional extent, shallow burial, large thickness (100–600 m), abundant OM, and moderate maturity. The findings of this investigation have implications for our understanding of pore generation in various OM materials. It is informative for Permian CBM reservoirs and has implications for evaluating gas exploration of the Permian coals and favourable intervals in the Damodar valley (Tripathy et al., 2018a, 2018b, 2019).

2 Methodology

Air-dried, finely crushed (<212 μm) coal samples were used for proximate analysis in accordance with ASTM guidelines. BET isotherms and hysteresis analysis were used to assess the pore size distribution, surface area, and pore morphology using low-pressure N_2 and CO_2 adsorption procedures. The Details of methodological procedure is provided in Tripathy et al., 2018c, Mazumder 2024a. Using the S_1, S_2, S_3, and T_{max} parameters, Rock-Eval pyrolysis was used to assess the amount, kind, and thermal maturity of organic matter. Reflected light microscopy was also used to estimate maceral composition and vitrinite reflectance ($R_{0,max}$), which provided information about coal petrography and maturity.

3 Result

The low-pressure liquid nitrogen adsorption experiment was used to determine the morphological characteristics of pore, including pore volume, specific surface area, and average pore diameter. Based on IUPAC classification, adsorption isotherm curves in Figure 1 (a). shows type B and type D hysteresis (Thommes et al., 2015). Barakar formation coal consists of slit shaped pore, whereas Raniganj formation coal contains bottle-neck pores.

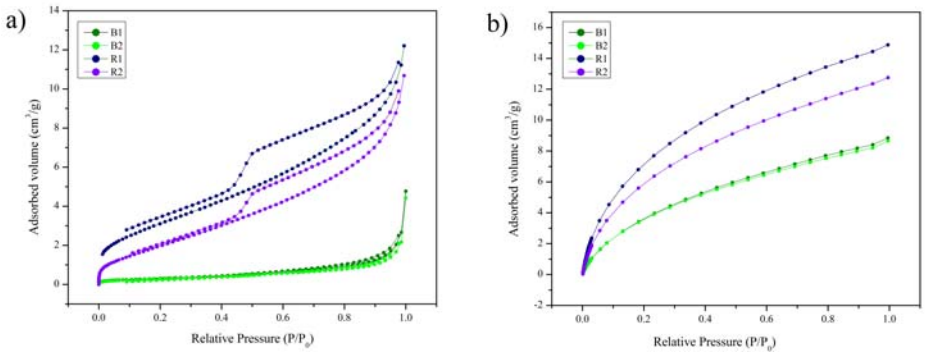


Fig. 1 Isotherm curves from LPGA a) LP-N_2 A isotherm curves. b) LP-CO_2 A isotherm curves.

Important metrics for describing reservoir characteristics and their adsorption capacity are the SSA and PV. SSA of samples ranges from 2.75 to 11.83 m^2/g whereas TPV of samples ranges between 0.003 to 0.02cm^3/g. Values of APD ranges from 6.39 to 24.9 nm. Figure 3 shows that the TPV and SSA have a significant positive correlation, whereas the TPV and SSA decrease as APD rises. This suggests that pores with lower APD create higher TPV and SSA (Chalmers et al., 2012; Yang et al., 2014; Fu et al., 2015; Liu et al., 2015). PSD of samples has been calculated based on BJH model (Xi et al., 2017). Samples from Barakar formation shows multimodal distribution, whereas Raniganj formation samples show bimodal distribution (Fig.2).

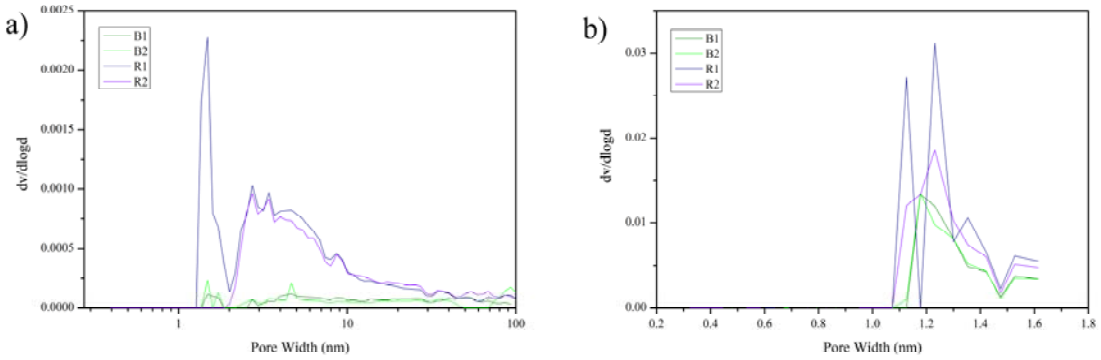


Fig. 2 PSD of coal samples based on LPGA. a) PSD from LP N_2 A. b) PSD from LP CO_2 A.

According to IUPAC, the adsorption curves from LP-CO_2 A in fig 1(b) exhibits the type I isotherm. Based on DFT model, pore characteristics of micropore has been determined. SSA ranges from 18.94 to 39.82 m^2/g and pore volume varies between 0.0089 to 0.0174cm^3/g. PSD of samples shows bimodal distribution.

The most crucial fractal theory parameter, fractal dimension D is computed by computing the various fractal models and is frequently used to quantitatively describe the roughness and structural complexity of pores. The Frenkel-Halsey-Hill (FHH) model is the three most often used fractal model.

Table 1 displays the Rock-eval pyrolysis parameters and TOC content of the samples under study. The average TOC content is with a range of 58.65% to 69.58%. T_{max} and R_0 (%) values of Barakar formation ranges from 462 to 481 °C and 1.14 to 1.24, and Raniganj formation coal varies between 422 and 426 °C and 0.63 to 0.68, indicating that Barakar coals are mature coal and Raniganj coals are immature coal (Pan et al., 2015).

Table 1. Rock eval pyrolysis data of coal.

Sample ID	TOC (wt %)	S1 (mg HC/g rock)	S2 (mg CO_2/g rock)	S3	Tmax (ºC)	HI (mg HC/g TOC)	OI
B1	58.65	1.30	123.89	0.43	481	211	0.78
B2	62.24	2.20	152.59	0.91	462	244	1.48
R1	69.58	0.43	250.23	1.30	422	359	2.98
R2	67.86	0.91	228.48	0	426	337	0.07

The range of vitrinite reflectance (R_0) of studied coal is from 0.66 to 1.2, as seen in Table 2, suggesting that the samples are sub-bituminous coal of middle rank. With a volume ranging from 46.0

to 67.0% (av. 57.5%), vitrinite dominates the coals, surpassing inertinite (15.0–38.0%, av. 25.25%) and liptinite (9.0–15.0%, av. 11.5%), as evidenced by table 2., which displays the maceral groups and elemental composition and fractal characteristics of the coals.

Table 2. Elemental composition, maceral contents and fractal characteristics of coal.

Sample ID	R_0 (%)	Moisture content (%)	Ash content (%)	Volatile matter (%)	Vitrinite (%)	Inertinite (%)	Liptinite (%)	D_{V1}	D_{V2}
B1	1.24	2.45	57.11	16.40	67	15	12	2.39	2.57
B2	1.14	2.29	53.42	19.23	62	17	15	2.3	2.68
R1	0.68	6.45	47.23	31.41	55	31	9	2.41	2.80
R2	0.63	5.35	47.01	35.47	46	38	10	2.21	2.75

4 Discussion

4.1 Effect of Organic Matter on Pore Development

Primary factors affecting the evolution of pore structure in CBM reservoirs during diagenesis are TOC content, kerogen type and degree of thermal maturity (Curtis et al., 2012; Ross and Bustin, 2009). Porosity in coal can be classified into organic and inorganic based on the origin. Secondary pores like OM pore are developed from kerogen during the generation of hydrocarbon. Some researchers suggested positive relationship between TOC and BET SSA, but in our study, TOC is negatively related with SSA. However, in case of samples containing TOC>10%, BET SSA shows a declining trend with increasing TOC. In our study, same thing has been noticed (Fig.3 (a)). Suggesting the contribution of factors other than organic matter in formation of pore.

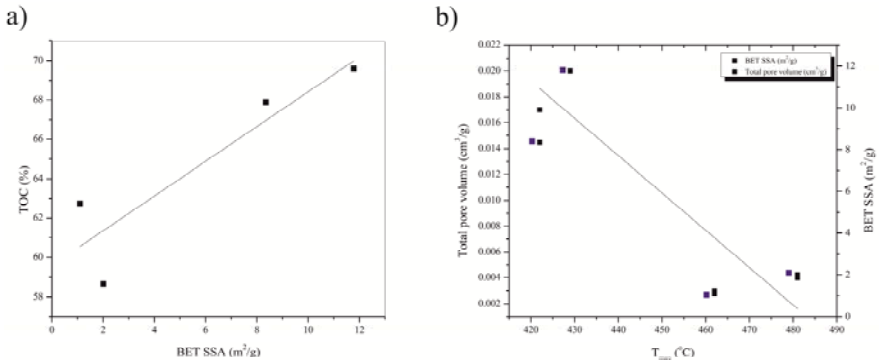


Fig. 3 a) Relationship between organic matter and BET SSA. b) Effect of T_{max} on pore parameters.

4.2 Effect of Thermal Maturity in Evolution of Pore Structure

Pore parameters are significantly affected by degree of thermal maturation. Fig. 3 (b) demonstrates that as Tmax increases, the TPV and SSA of coal's pore decrease. This suggests that as OM maturity rises, the development level of each type of pores decreases as well, leading to a drop in porosity and TPV in the over-mature stage. As graphitization in organic matter reduces the potentiality of hydrocarbon generation, it is responsible for the decrement in the proportion of organic matter.

4.3 Effect of Maceral Composition on pore parameters

Pore parameters can vary in different macerals within same coal. Fig. 4(a) shows inertinite content is positively associated with BJH TPV whereas vitrinite is negative correlated, suggesting that inertinite has greater effect on pore volume than vitrinite. Micropores generally develop in vitrinite, whereas macropores can be found in plant tissues like woody plant cell walls, within inertinite. So, in contrast with inertinite and liptinite, vitrinite has higher amount of micropores. Pore parameters can vary in different macerals within same coal. Fig. 4 (a) shows inertinite content is positively associated with BJH TPV whereas vitrinite is negative correlated, suggesting that inertinite has greater effect on pore volume than vitrinite.

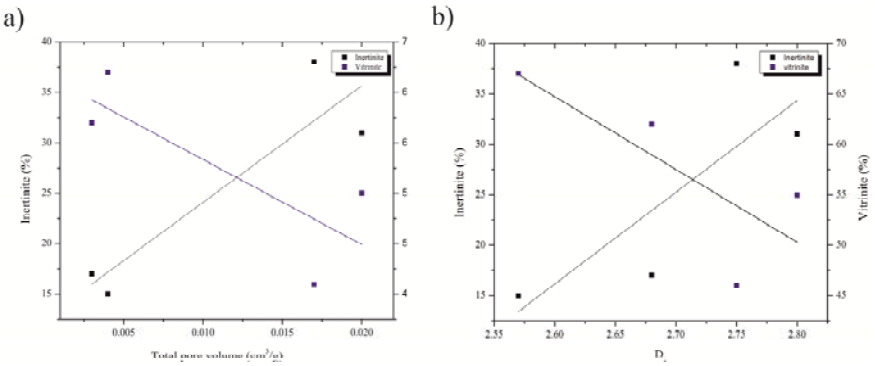


Fig. 4 a) Relationship between maceral contents and pore parameters. b) Relationship between maceral contents and fractal characteristics.

Fig. 4 (b) Coal's fractal dimension provides a thorough representation of its internal structure of pore. It also explains the relationship between complicacy of pore structure differs with different maceral compositions. Value of D_v increases with increasing inertinite content and decreases with increasing vitrinite content suggesting that pore morphology become complex with enrichment of inertinite in coal. However, no relationship has been observed between D_s and maceral composition.

5 Conclusion

- Low pressure N_2 adsorption analysis reveals that the majority of the pores in the coal samples from Raniganj formation are bottle-neck shaped, whereas Barakar formation coal mainly consists of slit shaped pores. The majority of pore volume is contributed by micropores, which make up 65.23% to 70.69%, followed by mesopore and macropore, respectively
- As BET SSA shows a declining trend with increasing TOC, suggesting the contribution of factors other than organic matter in the formation of pores.
- Vitrinite and inertinite have different pore structures with variety of pore size, which suggests a propensity for pore size alter. Inertinite content is positively related with total pore volume, whereas vitrinite is negatively associated with pore volume. Increment in values of D_v suggest that pore complexity gradually increases with increasing inertinite content.
- Outcomes of this study are particularly relevant to the characterization of Permian coalbed methane (CBM) reservoirs and have significant implications for assessing gas exploration potential in Permian coal fields.

References

Ardakani, O. H., Sanei, H., Ghanizadeh, A., Lavoie, D., Chen, Z., & Clarkson, C. R. (2018). Do all fractions of organic matter contribute equally in shale porosity? A case study from Upper Ordovician Utica Shale, southern Quebec, Canada. Marine and Petroleum Geology, 92, 794-808.https://doi.org/10.1016/j.marpetgeo.2017.12.009

Chalmers, G. R., Bustin, R. M., & Power, I. M. (2012). Characterization of gas shale pore systems by porosimetry, pycnometry, surface area, and field emission scanning electron microscopy/transmission electron microscopy image analyses: Examples from the Barnett, Woodford, Haynesville, Marcellus, and Doig units. *AAPG bulletin*, *96*(6), 1099-1119.DOI:10.1306/10171111052

Clarkson, C. R., Solano, N., Bustin, R. M., Bustin, A. M. M., Chalmers, G. R., He, L., ... & Blach, T. P. (2013). Pore structure characterization of North American shale gas reservoirs using USANS/SANS, gas adsorption, and mercury intrusion. Fuel, 103, 606-616.https://doi.org/10.1016/j.fuel.2012.06.119

Curtis, J. B. (2002). Fractured shale-gas systems. AAPG bulletin, 86(11), 1921-1938.

Curtis, M. E., Sondergeld, C. H., Ambrose, R. J., & Rai, C. S. (2012). Microstructural investigation of gas shales in two- and three-dimensions using nanometer-scale resolution imaging. AAPG bulletin, 96(4), 665-677. DOI:10.1306/08151110188

Du, X., Song, X., Zhang, M., Lu, Y., Lu, Y., Chen, P., ... & Yang, S. (2015). Shale gas potential of the Lower Permian Gufeng Formation in the western area of the Lower Yangtze Platform, China. *Marine and Petroleum Geology*, *67*, 526-543.https://doi.org/10.1016/j.marpetgeo.2015.05.031

Fu, H., Wang, X., Zhang, L., Gao, R., Li, Z., Xu, T., ... & Li, Q. (2015). Investigation of the factors that control the development of pore structure in lacustrine shale: a case study of block X in the Ordos Basin, China. *Journal of Natural Gas Science and Engineering*, *26*, 1422-1432.DOI:10.1016/j.jngse.2015.07.025

Jarvie, D. M., Hill, R. J., Ruble, T. E., & Pollastro, R. M. (2007). Unconventional shale-gas systems: The Mississippian Barnett Shale of north-central Texas as one model for thermogenic shale-gas assessment. *AAPG bulletin*, *91*(4), 475-499.DOI:10.1306/12190606068

Liu, B., Schieber, J., & Mastalerz, M. (2017). Combined SEM and reflected light petrography of organic matter in the New Albany Shale (Devonian-Mississippian) in the Illinois Basin: A perspective on organic pore development with thermal maturation. *International Journal of Coal Geology*, *184*, 57-72. DOI:10.1016/j.coal.2017.11.002

Liu, X., Xiong, J., & Liang, L. (2015).Investigation of pore structure and fractal characteristics of organic-rich Yanchang formation shale in central China by nitrogen adsorption/desorption analysis.*Journal of natural gas science and engineering*, *22*, 62-72.10.1016/j.jngse.2014.11.020

Loucks, R. G., Reed, R. M., Ruppel, S. C., & Hammes, U. (2012). Spectrum of pore types and networks in mudrocks and a descriptive classification for matrix-related mudrock pores. *AAPG bulletin*, *96*(6), 1071-1098.DOI:10.1306/08171111061

Loucks, R. G., Reed, R. M., Ruppel, S. C., & Jarvie, D. M. (2009). Morphology, genesis, and distribution of nanometer-scale pores in siliceous mudstones of the Mississippian Barnett Shale. *Journal of sedimentary research*, *79*(12), 848-861.doi.org/10.2110/jsr.2009.092

Mazumder, M., & Tripathy, A. (2024b). Study on the pore morphology and fractal features of coal from Raniganj coalfield, India using gas adsorption and FE-SEM analysis. In *New Challenges in Rock Mechanics and Rock Engineering* (pp. 909-914). CRC Press.

Mazumder, M., Bal, A., Tripathy, A., Liu, S., & Singh, T. N. (2024a). Multiscale Assessment of Transformation in Pore System of Shale during Combustion: An Insight into Poromechanical Response and Sorption Dynamics. *Energy & Fuels*, *38*(18), 17510-17524.doi.org/10.1021/acs.energyfuels.4c02383

Mazumder, M., Tripathy, A., & Singh, T. N. (2024c, January). Quantitative Evaluation of Sub-Bituminous Coal from Jharia Basin, India: Investigation Using Low Pressure N2 and CO2 Adsorption. In *International Conference on Geotechnical Issues in Energy, Infrastructure and Disaster Management* (pp. 649-658). Singapore: Springer Nature Singapore.

Milliken, K. L., Rudnicki, M., Awwiller, D. N., & Zhang, T. (2013). Organic matter–hosted pore system, Marcellus formation (Devonian), Pennsylvania. *AAPG bulletin*, *97*(2), 177-200.

Pan, L., Xiao, X., Tian, H., Zhou, Q., Chen, J., Li, T., & Wei, Q. (2015). A preliminary study on the characterization and controlling factors of porosity and pore structure of the Permian shales in Lower Yangtze region, Eastern China. *International Journal of Coal Geology*, *146*, 68-78.10.1016/j.coal.2015.05.005

Ross, D. J., & Bustin, R. M. (2009). The importance of shale composition and pore structure upon gas storage potential of shale gas reservoirs. *Marine and petroleum Geology*, *26*(6), 916-927.https://doi.org/10.1016/j.marpetgeo.2008.06.004

Thommes, M., Kaneko, K., Neimark, A. V., Olivier, J. P., Rodriguez-Reinoso, F., Rouquerol, J., & Sing, K. S. (2015). Physisorption of gases, with special reference to the evaluation of surface area and pore size distribution (IUPAC Technical Report). *Pure and applied chemistry*, *87*(9-10), 1051-1069.DOI 10.1515/pac-2014-1117

Tripathy, A., Srinivasan, V., & Singh, T. (2018a, April). Pore Size Distribution of shale using Advanced Analytical Techniques. In *EGU General Assembly Conference Abstracts* (p. 1010).

Tripathy, A., Srinivasan, V., & Singh, T. (2018b, June). Pore Characterization of Cambay Shale Using Low-pressure Gas Adsorption and MIP Analysis. In *80th EAGE Conference and Exhibition 2018* (Vol. 2018, No. 1, pp. 1-5). European Association of Geoscientists & Engineers.

Tripathy, A., Srinivasan, V., & Singh, T. N. (2018c). A comparative study on the pore size distribution of different Indian shale gas reservoirs for gas production and potential CO2 sequestration. *Energy & Fuels*, *32*(3), 3322-3334.DOI: 10.1021/acs.energyfuels.7b04137

Tripathy, A., Kumar, A., Srinivasan, V., Singh, K. H., & Singh, T. N. (2019). Fractal analysis and spatial disposition of porosity in major indian gas shales using low-pressure nitrogen adsorption and advanced image segmentation. *Journal of Natural Gas Science and Engineering*, *72*, 103009.10.1016/j.jngse.2019.103009

Wood, J. M., Sanei, H., Haeri-Ardakani, O., Curtis, M. E., Akai, T., & Currie, C. (2018). Solid bitumen in the Montney Formation: Diagnostic petrographic characteristics and significance for hydrocarbon migration. *International Journal of Coal Geology*, *198*, 48-62.

Xi, Z., Tang, S., Zhang, S., & Sun, K. (2017). Pore structure characteristics of marine–continental transitional shale: A case study in the Qinshui Basin, China. *Energy & Fuels*, *31*(8), 7854-7866.DOI: 10.1021/acs.energyfuels.7b0091

Yang, F., Ning, Z., & Liu, H. (2014). Fractal characteristics of shales from a shale gas reservoir in the Sichuan Basin, China. *Fuel*, *115*, 378-384.https://doi.org/10.1016/j.fuel.2013.07.040